

acting with the copper electrode. The equation obtained is

$$E^\infty/\text{mV} = 1003.6 - 1.5075T + 0.1340T \ln T - (16.9 \times 10^{-6})T^2 + 737.2/T \quad (14)$$

Similarly, on the basis of the above data, the thermodynamic quantities of other reactions involving copper chloride melts and the excess properties of these multicomponent mixtures could be evaluated. However, it must be remarked that all these data should be used only within the concentration range investigated and that extrapolations are only then accurate if the molten system  $\text{CuCl-CuCl}_2$  can be treated as an ideal mixture at the concerning concentrations.

#### Acknowledgment

I thank T. Ritterbex for his help in carrying out the experimental work.

Registry No.  $\text{CuCl}_2$ , 7447-39-4;  $\text{CuCl}$ , 7758-89-6.

#### Literature Cited

- (1) Chase, M. W., Jr.; Curnutt, J. L.; Downey, J. R., Jr.; McDonald, R. A.; Syverud, A. N.; Valenzuela, E. A. "JANAF Thermochemical Tables, 1982 Supplement"; *J. Phys. Chem. Ref. Data* **1982**, *11*, 695.
- (2) Wicks, C. E.; Block, F. E. "The Thermodynamic Properties of 65 Elements, Their Oxides, Halides, Carbides and Nitrides"; U.S. Government Printing Office: Washington, DC, 1963; *Bull.—U.S., Bur. Mines*, No. 605.
- (3) Barin, I.; Knacke, O. "Thermochemical Properties of Inorganic Substances"; Springer-Verlag: West Berlin, 1973.
- (4) Janz, G. J. "Molten Salt Handbook"; Academic Press: New York, 1967.
- (5) Hammer, R. R.; Gregory, N. W. *J. Phys. Chem.* **1964**, *68*, 3229.
- (6) Biltz, W.; Fischer, W. Z. *Anorg. Allg. Chem.* **1927**, *166*, 290.
- (7) Fontana, C. M.; Gorin, E.; Kidder, G. A.; Meredith, C. S. *Ind. Eng. Chem.* **1952**, *44*, 363.
- (8) Ruthven, D. M.; Kenney, C. N. *J. Inorg. Nucl. Chem.* **1968**, *30*, 931.
- (9) Sundermeyer, W. *Angew. Chem.* **1985**, *77*, 241.
- (10) Drossbach, P. Z. *Elektrochem.* **1952**, *56*, 23.
- (11) Giazitoglou, Z. *Ber. Bunsenges. Phys. Chem.* **1982**, *86*, 894.
- (12) Giazitoglou, Z. *Electrochim. Acta* **1983**, *28*, 491.

Received for review September 20, 1982. Accepted May 19, 1983. This work was supported by the German Research Partnership (Project SFB 163).

## Thermal Diffusion Factors near the Azeotrope Conditions of Ethanol–Water Mixtures

Edward R. Peterson, Tevln Vongvanich, and Richard L. Rowley\*

Department of Chemical Engineering, Rice University, Houston, Texas 77251

**A thermal diffusion column has been designed with unique sampling capabilities. This column has been used to investigate the behavior of the thermal diffusion factor, the thermal diffusion coefficient, and the corresponding Onsager coefficient in the azeotropic region of ethanol–water mixtures. In particular, the temperature dependence of these coefficients has been studied at 1 atm between 29 and 76 °C, to within 2 °C of the azeotrope point. Within statistical justification of the data, all three coefficients are linear. Experimental error increases near the azeotrope point, but it appears that no anomalous behavior due to azeotropic point proximity occurs; therefore, effective resolution of azeotropic mixtures can be made with thermogravitational techniques alone or in conjunction with distillation columns.**

#### Introduction

Thermal diffusion factors,  $\alpha_i$ , determine the magnitude of separations achieved at steady state by an applied temperature gradient. While thermal diffusion separations of liquid mixtures are not widely employed on a commercial scale due to the size of  $\alpha_i$ , there are important thermophysical property regions where thermal diffusion data may take on increased commercial significance and play an important role in elucidating the nature of liquid mixture interactions and resultant transport phenomena. For example, it has been shown that the thermal diffusion factor exhibits a "critical anomaly" or diverges as the temperature of a binary mixture approaches its liquid–liquid critical point or consolute temperature (1–4). Experiments indicate that this is due to the rapid decrease in magnitude of the diffusion coefficient thereby decreasing back-diffusion and enhancing dramatically the steady-state separation (3, 4). Similarly, near an azeotrope point, thermal diffusion data may

have an anomalous temperature dependence which would affect separations. Thermal diffusion could find application in conjunction with distillation columns, using the thermogravitational column to break the azeotrope (5). We report here the behavior of the thermal diffusion factor in ethanol–water mixtures of azeotrope composition as the temperature is increased to the azeotrope point.

#### Experimental Section

Horne and Bearman (6, 7) have shown that thermal diffusion factors can be obtained from thermogravitational columns by measuring steady-state separations using the equations

$$\alpha_1 = ABT\beta\Delta w_1/[w_1w_2(1-F)] \quad (1)$$

$$F = 19AB\rho(\bar{V}_2 - \bar{V}_1)\Delta w_1/1430 \quad (2)$$

$$B = \rho/\eta D \quad (3)$$

where  $A$  is a well-defined apparatus constant,  $w_i$  is the mass fraction of component  $i$ ,  $\Delta w_i$  is the steady-state composition difference between the top and the bottom of the column,  $\bar{V}_i$  is the partial specific volume of species  $i$ ,  $\rho$  is the density,  $\eta$  is the shear viscosity, and  $D$  is the mutual diffusion coefficient. Stanford and Beyerlein (8) have shown that thermogravitational columns without end reservoirs eliminate most end-effect problems and constitute an accurate reproducible means of determining thermal diffusion factors.

The column used in this work is shown schematically in Figure 1; the top seal, the sample tube arrangement, the column spacer, the vent, and the thermocouple wells are detailed in Figure 2. The column was made from three pieces of stainless-steel tubes of nominal o.d.'s and wall thicknesses 0.990, 1.135, 1.615 and 0.160, 0.187, and 0.175 in., respectively. After machining and straightening, this resulted in a

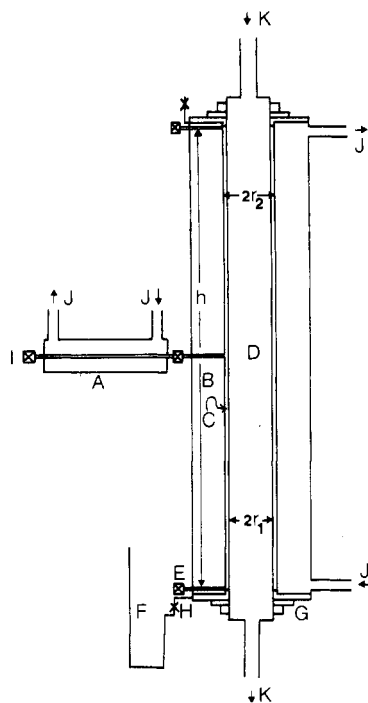


**Figure 1.** Thermogravitational column: (A) sampling heat exchanger, (B) outer jacket, (C) sample annulus, (D) inner jacket, (E) sample ports, (F) manometer, (G) end closure (see Figure 2), (H) filling port, (I) sampling input port, (J) outer jacket water flow (arrows show flow), (K) inner tube water flow. Column dimensions are  $h = 24.38 \pm 0.02$  cm,  $2r_1 = 2.217 \pm 0.003$  cm,  $2r_2 = 2.390 \pm 0.003$  cm, and an apparatus constant of  $A = (2r_1 r_2)^2 \ln(r_2/r_1)gh/63 = 200.2 \pm 0.2$  cm<sup>6</sup>/s<sup>2</sup>.

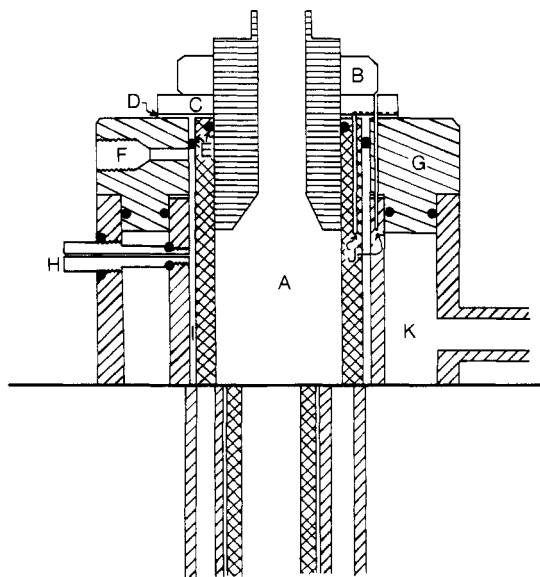


**Figure 2.** Expanded view of thermogravitational column end: (A) inner jacket, (B) sealing nut, (C) washer, (D) Teflon gasket and column spacer, (E) O-rings, (F) vent/filling port, (G) end cap, (H) sample port, (I) sample annulus, (J) thermocouple wells, (K) outer jacket.

thermogravitational column with the dimensions shown in Figure 1. The seal for the outside water jacket was made with a stainless-steel header-collar pressed between the middle and outer tubes. An O-ring recessed into the collar on either side forms the actual seal. The vent tube has a 1/16-in. LC port drilled through the collar at the very top of the annular sample ring. Closure of the sample space as well as spacing for the tubes is provided by a machined Teflon gasket as shown in Figure 2. The circular fin of this gasket fits tightly between the middle and inner tubes forming a spacer at both ends of the column. The actual liquid seal is formed by pressure of the fin portion of this gasket against an O-ring slightly recessed into

the outside wall of the middle tube. The assemblage is held together by a washer and nut at either end of the column threaded onto the inside tube and tightened against the Teflon gaskets. Small thermocouple wells were drilled in the walls of the inside and middle tubes at both the top and the bottom of the column. Thermocouple leads lie in a tiny slot cut on the underside of the washer and pass through their respective holes in the Teflon gasket and stainless-steel header in the case of outside probes. The wells are filled with mercury to aid response of the 0.4-mm-diameter measuring junctions, arc welded from precision 40-gage copper and constantan thermocouple wire.

Sample ports require two seals, one between the annular sample space and the outside water jacket and another between that jacket and the outside column. The sample ports were machined from stainless-steel rod with a 1/32-in. hole drilled through the center. The seal to the sample annulus is made with an O-ring seated into the wall of the middle tube which is compressed by turning the port until the threaded end of the port has seated into the threaded hole in the tube wall. This also locates the end of the port flush with the inside of the middle tube. The outside seal is then made with the compression of an O-ring by a nut threaded onto the outside of the sample port as shown in Figure 2. Soldered to the sample tubes are luer-loc valves for direct sampling with glass syringes.

The entire column was thermally insulated and mounted vertically by means of external clamps. Alignment was made by using a plumb line through the inside water tube before external Tygon tubing connections were made to the bath. High-grade thermocouple extension wires were used to connect the 40-gage calibrated measurement junctions to the ice point reference. Thermocouple leads extended within the wells in the walls to just below the fluid level. In this manner temperature measurements could be made on either the temperature difference across the annular space or the temperature drop down the length of the column. Water from baths, controlled internally to  $\pm 0.004$  °C, was circulated at a rate of 5 gal min<sup>-1</sup> to the column in a countercurrent arrangement to maintain a uniform temperature gradient. Differences in temperature between the top and the bottom of the column were generally less than 0.3 °C and the measured temperature differences across the sample at the top and the bottom agreed to within 0.03 °C.

The azeotrope mixture was prepared gravimetrically from Baker-analyzed anhydrous ethanol and doubly distilled-deionized water. Karl Fischer titration was used to determine the water content of the ethanol. Minute impurity effects upon the thermal diffusion factor were tested by performing thermal diffusion experiments on the absolute ethanol. No perceptible difference in refractive index was found between the absolute ethanol and steady-state samples obtained from the top and the bottom of the column. No further purification of the commercial absolute ethanol was performed.

A typical run consisted of azeotrope preparation, filling of the cell, application of the temperature gradient, establishment of steady state, and sampling. Most of these procedures are typical of thermogravitational column operational techniques (9); only unique items will be discussed here.

Filling of the column was done through the bottom 1/16-in. line with the vent, located at the extreme top to allow displacement of all air bubbles, open. The bottom fill line was connected to a narrow-bore, open-end mercury manometer; all air between the sample and the mercury was withdrawn through a three-way luer-loc valve. Filling of the column was done at run temperature. Once the column was completely filled, liquid azeotrope was alternately infused from the bottom and top vent/filling ports to eliminate any bubbles. The connection to the manometer was left open during the fluid heat-up period to allow for thermal expansion of the liquid. When the

thermocouple readings had reached steady-state values, the excess mixture was drained from the U-tube until the mercury level was restored to the original level. The connection to the manometer was made with 1/64-in.-i.d. stainless-steel tubing to minimize dead volume external to the column while still providing the means for reestablishment of ambient pressure in the column following initial fluid warm-up.

While only a few experimental steady-state time determinations were performed, a theoretical estimate was obtained (9). Generally a factor of 3 or more was included in these estimates to ensure complete steady-state operation; samples were often allowed to remain in the column under run conditions for 24–36 h to ensure establishment of the steady-state concentration profile.

While common sampling procedure consists of withdrawing samples through a port with a vent open to the column, the moisture-sensitive nature of our system prohibited the introduction of displacement air. We chose instead to infuse a small amount of the azeotrope mixture into the center of the column to displace a bottom and top sample into cool syringes. Whereas some previous work has required relatively large sample volumes for analysis purposes, we used a flow differential refractometer which required only 10- $\mu$ L samples. This has the advantage that no linear estimate of the effect of sample size on the measured  $\Delta w_1$  need be performed, eliminating one possible source of systematic error. In practice, each sample line was first purged with about 0.1 mL and then a 0.1–0.2-mL sample was withdrawn from each of the top and bottom ports in that order. This was repeated at least 3 times. No systematic sample volume error was detected until the fourth samples from the top and bottom port were obtained. In no case were sample volumes larger than 0.3 mL (less than 2% of the column volume). This sampling procedure required infusion of fresh azeotrope mixture at column half-height where the steady-state composition is approximately that of the azeotrope. It is therefore important that the density of the infused liquid be nearly the same as that of the fluid at the center of the column, otherwise convection patterns will disturb the samples withdrawn. To prevent large density differences between the displacement mixture and the fluid in the column, a heat exchanger was added to the central port. The 1/16-in.-o.d. stainless-steel infusion line was jacketed with an insulated 1/2-in. copper tube to create a double pipe heat exchanger. As the samples were taken from the top and the bottom of the column by displacement, the entering fluid was heated to column temperatures by slow infusion through the heat exchanger. Results with and without the heat exchanger were consistent at lower column temperatures, when the difference in temperature between the displacement fluid and the column fluid was less than about 15 °C. For column temperatures closer to the azeotrope temperature of 78.17 °C, the heat exchanger was indispensable; without it, refractometer peaks were partially attenuated and exhibited rather random magnitudes and anomalous shapes. The consistency of the results obtained by using this sampling technique as opposed to air displacement is evidence in support of this technique for columns operated at temperature conditions quite different from ambient.

Compositions of samples were determined with a Perkin-Elmer Model 1107 differential flow refractometer with a resolution of  $10^{-6}$  refractive index unit. Freshly prepared azeotrope mixture was infused through both the reference and sample prisms by a two-channel syringe pump. Prisms and flow lines were thermostated to  $25.000 \pm 0.005$  °C. A chromatographic switching valve with a 10- $\mu$ L loop capacity was used for injecting a plug of mixture for analysis into the sample flow line. Peak heights were measured from the strip chart tracing of the response. Differences in composition from the azeotrope were

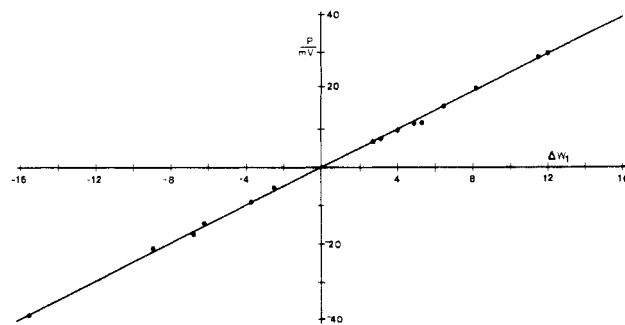


Figure 3. Calibration curve for ethanol (1)–water (2) mixtures relative to the azeotrope composition.

Table I. Results of Steady-State Thermogravitational Separations of Ethanol (1)–Water (2) Mixtures Containing  $95.60 \pm 0.001$  wt % Ethanol

$\langle T \rangle$ , °C	$\Delta T$ , °C	$10^3 w_1$	$\delta$	$\alpha_1$ <sup>a</sup>
28.96	2.49	4.92	0.04	2.07
33.06	2.98	4.84	0.09	2.07
36.86	4.00	4.68	0.13	2.03
39.49	4.40	4.76	0.17	2.08
43.97	4.21	4.05	0.07	1.78
48.22	1.56	3.52	0.01	1.55
52.58	2.84	3.29	0.04	1.45
55.26	3.49	2.97	0.10	1.31
56.95	2.61	3.21	0.03	1.42
61.09	5.22	3.22	0.07	1.43
63.54	3.97	3.13	0.08	1.39
65.73	4.23	3.03	0.09	1.35
69.76	4.80	2.70	0.13	1.23
71.97	4.34	2.53	0.36	1.17
74.36	3.95	2.40	0.10	1.13
75.16	2.57	2.77	<sup>b</sup>	1.31
76.01	2.30	2.60	0.10	1.24
76.23	2.67	2.50	0.33	1.20

<sup>a</sup>  $s = 0.115$ ,  $r = -0.942$ .  $s$  is the standard error of the estimate;  $r$  is the correlation coefficient. <sup>b</sup> Only one analysis was performed.

found from the refractometer voltage output by comparison to a calibration curve obtained from samples gravimetrically prepared. The calibration data obtained and a resultant least-squares fit are shown in Figure 3. The solid line represents the equation

$$10^3 \Delta w_1 = 0.4072P \quad (4)$$

fitted with a correlation coefficient of 0.996, where  $\Delta w_1$  is the difference in weight fraction from the azeotrope composition of 0.9560 and  $P$  is the peak height output in millivolts. Calibration of the column itself was made with the cyclohexane–benzene system. Literature values (10) compared favorably with our results within a 10% experimental accuracy.

## Results and Discussion

Experiments were performed on ethanol (1)–water (2) mixtures at the azeotrope composition ( $w_1 = 0.9560$ ) over the temperature range 29–76 °C with emphasis on data in the azeotrope region ( $T_{az} = 78.14$  °C) (11). The resultant data are shown in Table I, each point corresponding to two to four samples withdrawn from the column. The standard deviations displayed in column four of Table I were computed from the analysis of these multiple samples. Thermal diffusion factors,  $\alpha_1$ , were then computed from the observed separations using eq 1–3 and the thermophysical property data of Table II. Literature data for the thermophysical properties (12–18) were fitted to the polynomials shown in Table II with a multiple regression program designed to test for the statistical significance of each term with an  $F$  test.

Table II. Thermophysical Properties Used To Obtain  $\alpha_1$ 

property	equation <sup>a</sup>	ref
$\rho/(\text{kg L}^{-1})$	$0.82007 - (8.756 \times 10^{-4})T$	12-14
$\beta/\text{K}$	$8.756 \times 10^{-4}/\rho$	12-14
$\eta/(\text{kg m}^{-1} \text{s}^{-1})$	$10^{-3}\{2.2904 - 0.05785T + (7.353 \times 10^{-4})T^2 - (3.818 \times 10^{-6})T^3\}$	15-17
$D/(\text{m}^2 \text{s}^{-1})$	$10^{-9}\{0.7431 + (6.086 \times 10^{-3})T + (2.935 \times 10^{-4})T^2\}$	18
$(\bar{V}_1 - \bar{V}_2)/(\text{L mol}^{-1})$	$-0.4417 - (1.012 \times 10^{-5})T^2$	12-14

<sup>a</sup>  $T$  is in degrees Celsius.

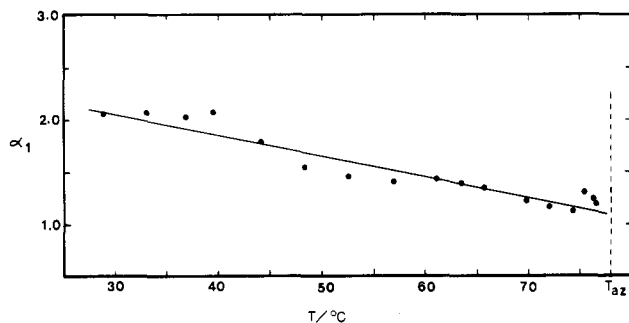


Figure 4. Thermal diffusion factors,  $\alpha_1$ , for the 95.60% ethanol-water mixture as a function of temperature. The azeotrope temperature is labeled  $T_{az}$ .

There is a definite decrease in  $\alpha_1$  as the temperature is increased toward the azeotrope temperature as seen from Figure 4. Experiments could not be performed much closer to the azeotrope temperature than about 76.3 °C without greatly diminishing the applied temperature gradient. This in turn causes problems with accuracy in composition analyses. However, with the possible exception of the very near azeotrope region, it appears that  $\alpha_1$  is well represented by the linear equation

$$\alpha_1 = 2.666 - 0.0202T(^{\circ}\text{C}) \quad (5)$$

over the temperature range which we have investigated. The correlation coefficient and the standard error for this fit are -0.942 and 0.11, respectively.

While the thermal diffusion factor does not apparently show any anomalous behavior near the azeotrope point, it does remain reasonably large even within 2 °C of the azeotrope. Azeotropic mixtures of ethanol and water can therefore be partially separated by thermal diffusion. We have performed a set of operations in which the azeotrope mixture is fed to a thermal diffusion column and the top product, enriched in ethanol, is then further distilled to obtain absolute ethanol. The net result is distillation using thermal diffusion to break the azeotrope. While this method works on a small scale, larger applications would require cascaded thermal diffusion columns to remove the top product far enough from the azeotropic composition to make further distillation practical.

Thermal diffusion factors can be related to other transport properties through various identities. Of particular interest in our work are Onsager coefficients as obtained from the nonequilibrium thermodynamics formulations of transport phenomena. The Onsager cross coefficient relating heat and mass transport in a binary system,  $\Omega_{10}$ , can be related to the thermal diffusion factor by

$$\Omega_{10} = \rho D w_1 w_2 \alpha_1 \quad (6)$$

Often the thermal diffusion coefficient,  $D_T$ , is reported rather than  $\alpha_1$ ; the two are related by

$$D_T = w_1 w_2 D \alpha_1 \quad (7)$$

Using the properties of Table II and the results of our experiments, we have determined  $\Omega_{10}$  and  $D_T$  and their temperature

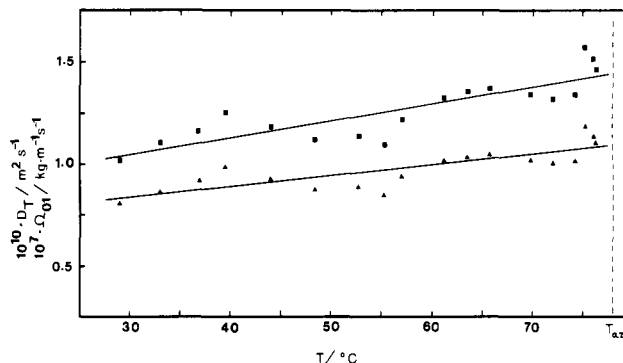


Figure 5. Thermal diffusion coefficients,  $D_T$  (■), and Onsager coefficients,  $\Omega_{10}$  (▲), as a function of temperature for 96.60% ethanol-water mixtures;  $T_{az}$  represents the azeotrope temperature.

dependences near the azeotrope point as shown in Figure 5. Though there is no theoretical reason why  $\alpha_1$ ,  $D_T$ , and  $\Omega_{10}$  should be a linear function of temperature, a straight-line behavior represents the data within the statistically allowed precision. The equations obtained for  $D_T$  and  $\Omega_{10}$  are

$$10^{10} D_T = 0.794 + 0.00794T(^{\circ}\text{C}) \text{ m}^2 \text{ s}^{-1}$$

$$10^7 \Omega_{10} = 0.671 + 0.00538T(^{\circ}\text{C}) \text{ kg m}^{-1} \text{ s}^{-1} \quad (8)$$

with correlation coefficients of 0.848 and 0.803, respectively.

As the azeotrope temperature is approached, the applied temperature gradient was necessarily smaller. This caused a decrease in the steady-state separation and therefore a small increase in the relative uncertainty of  $\alpha_1$  due to a fixed accuracy in our analytical technique. As can be seen from Table I, there is a noticeable increase in the uncertainty of the data as the azeotropic boiling point is approached. Only a small portion of this uncertainty increase is associated with the decreased temperature field applied; most can be ascribed to sampling difficulties for this specific system. For example, the enriched alcohol samples are hygroscopic and care must be used in sampling and handling. Furthermore, very near the boiling point there may be flashing or vaporization problems if samples are not carefully obtained.

## Conclusions

We have measured thermal diffusion factors as a function of temperature in mixtures of ethanol and water at the azeotropic composition. While the direction of the separation is consistent with earlier studies (19), we have elucidated the quantitative nature of the thermal diffusion factor near the azeotropic boiling point. In particular, no anomalous behavior occurs as the temperature is increased, the thermal diffusion factor is a linear function of temperature, and separations based on using a thermogravitational column to break the azeotrope are possible. An improved method of sampling thermogravitational columns was also developed. A small amount of the initial charge thermostated to column conditions can be injected at the center of the column to displace the sample at either end of the column. This eliminates problems which can occur in columns designed to use air displacement sampling techniques.

Registry No. Ethanol, 64-17-5.

### Literature Cited

- (1) Haase, R.; Bienert, B. K. *Ber. Bunsenges. Phys. Chem.* **1966**, *71*, 392-7.
- (2) Haase, R. *Ber. Bunsenges Phys. Chem.* **1972**, *76*, 258-9.
- (3) Giglio, M.; Vendramini, A. *Phys. Rev. Lett.* **1975**, *34*, 561-4.
- (4) Rowley, R. L.; Horne, F. H. *J. Chem. Phys.* **1979**, *71*, 3841-50.
- (5) Begeman, C. R.; Cramer, P. L. *Ind. Eng. Chem.* **1955**, *47*, 202-8.
- (6) Horne, F. H.; Bearman, R. J. *J. Chem. Phys.* **1967**, *46*, 4126-44.
- (7) Horne, F. H.; Bearman, R. J. *J. Chem. Phys.* **1968**, *49*, 2457-9.
- (8) Stanford, D. J.; Beyerlein, A. *J. Chem. Phys.* **1973**, *58*, 4338-43.
- (9) Powers, J. E. "New Chemical Engineering Separations"; Schoen, H. M., Ed.; Interscience: New York, 1962; Chapter 1.
- (10) Story, M. J.; Turner, J. C. R. *Trans. Faraday Soc.* **1969**, *65*, 349-51.
- (11) Horsley, L. H., Ed. "Azeotropic Data—III"; American Chemical Society: Washington, DC, 1973; *Adv. Chem. Ser.* Vol. 116.
- (12) Washburn, E. W. "International Critical Tables", 1st ed; McGraw-Hill: New York, 1928; Vol. 3, p 116-7.
- (13) Manabe, M.; Koda, M. *Bull. Chem. Soc. Jpn.* **1975**, *48*, 2367-71.
- (14) Friedman, M. E.; Scheraga, H. A. *J. Phys. Chem.* **1965**, *69*, 3795-800.
- (15) Smith, I. E.; Storrow, J. A. *J. Appl. Chem.* **1952**, *2*, 225-35.
- (16) Pratt, K. C.; Wakeham, W. A. *Proc. R. Soc. London, Ser. A* **1974**, *336*, 393-406.
- (17) Tyn, M. T.; Calus, W. F. *J. Chem. Eng. Data* **1975**, *20*, 310-6.
- (18) Vargaftik, N. B. "Tables on the Thermophysical Properties of Liquids and Gases", 2nd ed.; Hemisphere Publishing Co.: Washington, DC, 1975.
- (19) Jones, A. L.; Milberger, E. C. *Ind. Eng. Chem.* **1953**, *45*, 2689-96.

Received for review November 24, 1982. Accepted May 16, 1983. Support of a portion of this work by the Robert A. Welch Foundation grant no. C-801 is gratefully acknowledged.

## Protonation Constants of Mono-, Di-, and Triethanolamine. Influence of the Ionic Composition of the Medium

Juan M. Antelo, Florencio Arce, Julio Casado,\* Manuel Sastre, and Angel Varela

Departamento de Química Física, Facultad de Química, Departamento de Investigaciones Químicas, C.S.I.C., Universidad de Santiago de Compostela, Spain

The ionization constants in aqueous solution of mono-, di-, and triethanolamine were determined potentiometrically at 25 °C for ionic strengths ranging from 0.05 to 1.5 M, the inert electrolyte being KCl, KBr, or KNO<sub>3</sub>. A linear relationship was found to hold between pK and  $I^{1/2}$ . The thermodynamical constants have been calculated.

### Introduction

The properties of alkanolamines, including their important capacity for removing acidic components from natural and refinery gases, depend among other factors on their basic nature. Although values have been published for the ionization constants of alkanolamines at various temperatures and in various solvents (1-5), we are aware of no systematic study of the effect of the ionic composition of the medium. To fill this gap the present article describes a study of the influence of the nature and concentration of the inert electrolyte upon the ionization constants of protonated monoethanolamine (MEA), diethanolamine (DEA), and triethanolamine (TEA), i.e., upon the constants corresponding to the process  $AH^+ \rightleftharpoons A + H^+$ . The corresponding thermodynamical constants have also been calculated.

### Experimental Section

All the chemical products employed were Merck p.a. The ionization constants of protonated MEA, DEA, and TEA were determined by titrating aqueous solutions of the alkanolamines with hydrochloric acid at various ionic strengths (0.05, 0.10, 0.25, 0.50, 1.00, and 1.50 M) and with various inert electrolytes (KCl, KBr, and KNO<sub>3</sub>). The thermostated titration cell had inlets for the microburet, a current of nitrogen, a thermometer, and an electrode. pH was measured with a Beckman 4500 pH-meter accurate to 0.001 pH unit and Radiometer GK2401C electrode. The pH-meter was calibrated before each titration by using Beckman buffer solutions of pH 7 and 10. The titration curves from which the protonation constants of the alkanolamines are calculated lie within this pH range. The temperature

Table I. Ionization Constants of Protonated MEA, DEA, and TEA at  $T = 25^\circ\text{C}$

$I/M$	$pK_{\text{exptl}}$		
	KBr	KCl	KNO <sub>3</sub>
Monoethanolamine			
1.50	9.86 ± 0.01	9.87 ± 0.01	9.83 ± 0.01
1.00	9.81 ± 0.01	9.81 ± 0.01	9.79 ± 0.01
0.50	9.75 ± 0.01	9.74 ± 0.01	9.74 ± 0.01
0.25	9.72 ± 0.01	9.70 ± 0.01	9.69 ± 0.01
0.10	9.64 ± 0.01	9.67 ± 0.01	9.65 ± 0.01
0.05	9.65 ± 0.02	9.65 ± 0.01	9.60 ± 0.01
0.00 <sup>a</sup>	9.58 ± 0.02	9.60 ± 0.01	9.59 ± 0.02
Diethanolamine			
1.50	9.37 ± 0.01	9.40 ± 0.01	9.33 ± 0.01
1.00	9.31 ± 0.01	9.33 ± 0.01	9.27 ± 0.01
0.50	9.19 ± 0.01	9.23 ± 0.01	9.18 ± 0.01
0.25	9.11 ± 0.01	9.15 ± 0.01	9.12 ± 0.01
0.10	9.05 ± 0.01	9.10 ± 0.01	9.06 ± 0.01
0.05	9.02 ± 0.01	9.02 ± 0.01	9.02 ± 0.01
0.00 <sup>a</sup>	8.96 ± 0.03	8.97 ± 0.02	8.96 ± 0.01
Triethanolamine			
1.50	8.31 ± 0.01	8.27 ± 0.01	8.19 ± 0.01
1.00	8.18 ± 0.01	8.21 ± 0.01	8.13 ± 0.01
0.50	8.04 ± 0.01	8.10 ± 0.01	8.05 ± 0.01
0.25	7.99 ± 0.01	8.00 ± 0.01	8.02 ± 0.01
0.10	7.93 ± 0.01	7.96 ± 0.01	7.96 ± 0.01
0.05	7.89 ± 0.01	7.96 ± 0.01	7.92 ± 0.01
0.00 <sup>a</sup>	7.80 ± 0.02	7.86 ± 0.02	7.87 ± 0.01

<sup>a</sup> Extrapolated value.

of all experiments was maintained at  $25 \pm 0.1^\circ\text{C}$  by water flow from a thermostat.

### Results and Discussion

The pK was calculated by using the equation

$$pK_{\text{exptl}} = \text{pH} - \log \left[ \frac{B_0}{c_0 V + [(K_w)(10^{\text{pH}}) - 10^{-\text{pH}}](V_0 + V)} - 1 \right] \quad (1)$$